ENEA Ricerca Sistema Elettrico	Sigla di identificazione	Distrib.	Pag.	di
	ADPFISS-LP1-064	L	1	40

Titolo

Preliminary Results of the BUGJEFF311.BOLIB Library Validation on the Iron-88 (Fe) Neutron Shielding Benchmark Experiment

Descrittori

Tipologia del documento: Rapporto tecnico

Collocazione contrattuale: Accordo di programma ENEA-MSE su sicurezza nucleare e reattori di IV generazione

Argomenti trattati: Fisica nucleare, dati nucleari, fisica dei reattori nucleari

Sommario

Preliminary results concerning the ENEA-Bologna BUGJEFF311.BOLIB working cross section library validation on the Iron-88 single material (iron) integral neutron shielding benchmark experiment are presented. The BUGJEFF311.BOLIB library is specifically dedicated to LWR shielding and pressure vessel dosimetry applications. It is a broad-group coupled (47 n + 20 γ) working library in FIDO-ANISN format, based on the OECD-NEADB JEFF-3.1.1 evaluated nuclear data library and with the same group structure as the ORNL BUGLE-96 similar library. The analysis of the Iron-88 Winfrith benchmark experiment was performed through 3D transport calculations in Cartesian geometry using the ORNL TORT-3.2 discrete ordinates (S_N) code, the BUGJEFF311.BOLIB library and the threshold activation dosimeter cross sections for Rh-103(n,n')Rh-103m, In-115(n,n')In-115m, S-32(n,p)P-32 and Al-27(n,α)Na-24, derived from the IAEA IRDF-2002 reactor dosimetry file.

Note

Authors: Massimo PESCARINI, Roberto ORSI

Copia n.			In carico a:			
2			NOME			
			FIRMA			
1			NOME			
			FIRMA			
0	EMISSIONE	28/06/2016	NOME	M. Pescarini	F. Padoani	E. De Rosa
			FIRMA	M. Pescarini	F. Padoani	E. De Rosa
REV.	DESCRIZIONE	DATA		REDAZIONE	CONVALIDA	APPROVAZIONE

INDEX

Preliminary Results of the BUGJEFF311.BOLIB Library Validation on the Iron-88 (Fe) Neutron Shielding Benchmark Experiment

Massimo PESCARINI, Roberto ORSI

June 2016

1 - INTRODUCTION

The ENEA-Bologna Nuclear Data Group performed further validation of the ENEA-Bologna BUGJEFF311.BOLIB /1/ working cross section library for LWR shielding and pressure vessel dosimetry applications on the Iron-88 /2/ single material (iron) neutron shielding benchmark experiment. Iron-88 is in particular included in the SINBAD REACTOR /3/ /4/ database of neutron shielding benchmark experiments, dedicated to nuclear fission reactors. The analysis of the Iron-88 (Winfrith, UK) benchmark experiment was performed through three-dimensional (3D) transport calculations using the ORNL TORT-3.2 /5/ discrete ordinates (S_N) transport code, the BUGJEFF311.BOLIB library and the threshold activation dosimeter cross sections for Rh-103(n,n')Rh-103m, In-115(n,n')In-115m, S-32(n,p)P-32 and Al-27(n,α)Na-24, derived from the IAEA IRDF-2002 /6/ reactor dosimetry file.
BUGJEFF311.BOLIB is in particular a broad-group coupled neutron/photon (47 n + 20 γ) working cross section library in FIDO-ANISN /7/ format, based on the OECD-NEADB JEFF-3.1.1 /8/ /9/ evaluated nuclear data library and characterized by the same group structure as the ORNL BUGLE-96 /10/ similar library, specifically recommended by the American National Standard /11/ of the American Nuclear Society “Neutron and Gamma-Ray Cross Sections for Nuclear Radiation Protection Calculations for Nuclear Power Plants” (ANSI/ANS-6.1.2-1999, R2009) for LWR shielding and radiation damage applications. A preliminary comparison of the calculated and experimental reaction rates for the cited threshold activation dosimeters is presented.

2 - THE IRON-88 NEUTRON SHIELDING BENCHMARK EXPERIMENT

The ASPIS shielding facility of the Winfrith NESTOR reactor, the Iron-88 benchmark experimental array, the activation detector measurements and the fission plate neutron source are described, taking the relative information integrally from reference /2/ and from the document of the Iron-88 section of SINBAD REACTOR /3/, entitled “General Description of the Experiment”.

2.1 The ASPIS Shielding Facility

The ASPIS shielding facility is installed on the NESTOR reactor at Winfrith. NESTOR is a light water cooled, graphite and light water moderated reactor which operates at powers of up to 30 kW and is used as a source of neutrons for a wide range of applications. The core of the reactor, which comprises 26 MTR (Materials Test Reactor) type fuel elements, is contained within an annulus formed by two concentric aluminium vessels through which water

circulates. The inner vessel is filled with graphite to form an inner reflector. The outer tank is surrounded by an external graphite reflector in the form of a block having dimensions 182 cm × 182 cm × 122 cm which contains the control plate slots adjacent to the vessel wall. Leading off each of the four faces of the external reflector is an experiment cave which can be isolated from the reactor by shutters composed of boral or combinations of neutron/gamma-ray shield materials. ASPIS is located in the NESTOR cave C. Shield components, which are in the main slabs or tanks, are mounted vertically in a mobile tank which has an internal cross-sectional area of 1.8 m × 1.9 m and a length of 3.7 m. A fission plate is located within the experimental shield array. The loaded tank is moved into the cave where thermal neutrons leaking from the outer graphite reflector of NESTOR are used to drive the fission plate to provide a well defined neutron source for penetration measurements. The neutron flux levels within an ASPIS shield contain contributions from sources in the fission plate and from the NESTOR core and it is essential that the NESTOR contribution is subtracted from all measured responses to arrive at the response resulting from the fission plate sources.

2.2 - The Iron-88 Benchmark Experimental Array

The Iron-88 benchmark experimental array irradiated in the ASPIS shielding facility is shown schematically in side elevation in Figure 1. The array comprises three regions; the source region containing moderator and the fission plate, the shield made from 13 mild steel plates, each of approximately 5.1 cm thickness, and a deep backing shield manufactured from mild and stainless steel. To allow detector access within the shield, 6 mm spacers are placed between each slab component. In practice the depth of the air gaps varies owing to positional uncertainties of the plates and their flatness. The 6 mm gap is therefore nominal and an average gap of 7.4 mm was measured for the experiment. The axial dimensions of the experimental components are given in Table 1. The outer boundaries of the experimental region are formed by the walls and floor of the ASPIS trolley and by the roof of the ASPIS cave. The floor and walls of the trolley are manufactured from 1.91 cm thick mild steel plate. The trolley base has a 25 cm high steel chassis in-filled with concrete. The structure of NESTOR surrounding the trolley comprises concrete bulk shielding blocks except on the NESTOR core side of the trolley front face where it is graphite. This graphite extends away from the trolley to the external graphite reflector of the reactor. Table 2 gives the compositions of the materials used in the experiment.

Figure 1 Schematic side elevation of the shield in the iron 88 single material benchmark experiment

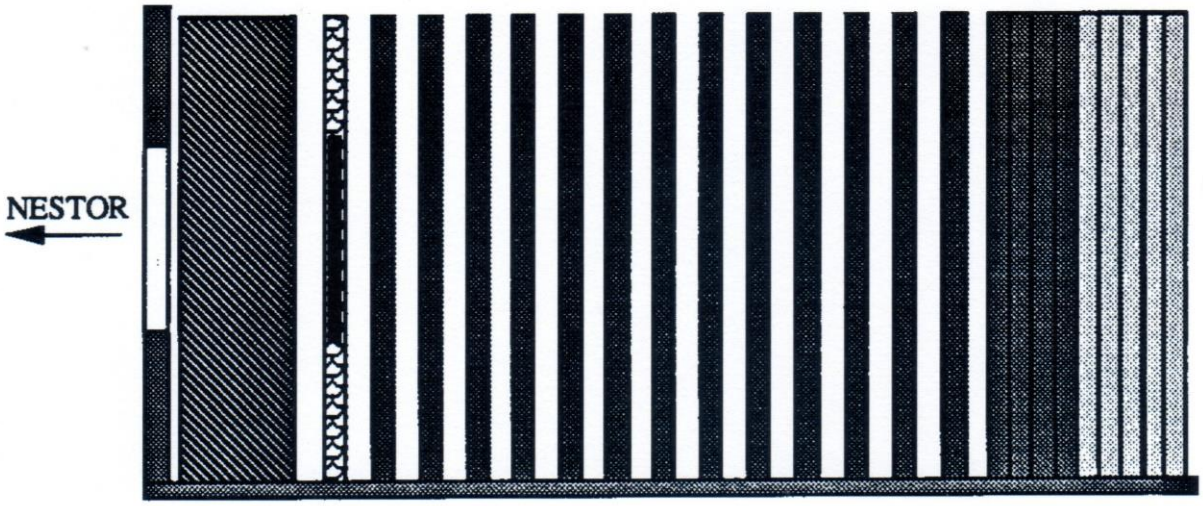

KEY

- Fuel
- Mild Steel
- Stainless Steel
- Fission Plate
- Graphite
- Aluminium

All components are 182.9cm wide by 191.0cm high

Not To Scale

Table 1

Shield Dimensions of the Iron-88 Single Material Benchmark Experiment.

Component	Mat.Thickness (cm)	Coordinate at End of Region (cm)	Mat. Reference Number
Trolley Face	3.18	-16.62	1 & 2
Void	0.52	-16.10	-
Graphite	15.00	-1.10	3
Void	1.10	0.00	-
Fission Plate	2.90	2.90	4 & 5
Void	0.74	3.64	-
Mild Steel	5.10	8.74	6
Void	0.74	9.48	-
Mild Steel	5.12	14.60	6
Void	0.74	15.34	-
Mild Steel	5.12	20.46	6
Void	0.74	21.20	-
Mild Steel	5.10	26.30	6
Void	0.74	27.04	-
Mild Steel	5.20	32.24	6
Void	0.74	32.98	-
Mild Steel	5.15	38.13	6
Void	0.74	38.87	-
Mild Steel	5.20	44.07	6
Void	0.74	44.81	-
Mild Steel	5.20	50.01	6
Void	0.74	50.75	-
Mild Steel	5.25	56.00	6
Void	0.74	56.74	-
Mild Steel	5.18	61.92	6
Void	0.74	62.66	-
Mild Steel	5.07	67.73	6
Void	0.74	68.47	-
Mild Steel	5.12	73.59	6
Void	0.74	74.33	-
Mild Steel	5.18	79.51	6
Void	0.74	80.25	-
Mild Steel	5.10	85.35	6
Mild Steel	5.25	90.60	6
Mild Steel	5.00	95.60	6
Mild Steel	4.67	100.27	6
Stainless Steel	22.41	122.68	7
Concrete	100.00	222.68	8

Notes

1. **For material compositions see Table 2.**
2. **The trolley face is manufactured from mild steel with a central aluminium 'window' of radius 56.1 cm.**
3. **The construction of the fission plate is shown in Figure 5.**
4. **All slab components are 182.9 cm wide by 191.0 cm high and fill the full width and height of the ASPIS trolley.**

Table 2

Material Compositions in the Iron-88 Single Material Benchmark Experiment.

Material	Material Ref. No.	Density (g/cm^3)	Element	Weight Fraction
Mild Steel	1	7.835	Fe	0.9865
			Mn	0.0109
			C	0.0022
			Si	0.0004
Aluminium	2	2.700	Al	1.0000
Graphite	3	1.650	C	1.0000
Fuel	4	3.256	Al	0.7998
			U-235	0.1864
			U-238	0.0138
Aluminium	5	2.666	Fe	0.0056
			Si	0.0015
			Al	0.9929
Mild Steel	6	7.850	Fe	0.9903
			Mn	0.0074
			C	0.0023
Stainless Steel	7	7.917	Fe	0.6695
			Mn	0.0157
			Cr	0.1677
			Ni	0.1166
			C	0.0006
			Si	0.0050
			P	0.0003
			S	0.0002
			Mo	0.0244
Concrete	8	2.242	Fe	0.0141
			Si	0.3369
			Al	0.0340
			H	0.0100
			O	0.5290
			Ca	0.0379
			K	0.0200
			Na	0.0161

2.3 - Activation Detector Measurements

The neutron distribution through the experimental shield has been mapped using activation foils attached to thin aluminium carriers (0.5 mm thick by 9 cm wide) located between the slab components. The detector set comprised activation foils to measure the epi-cadmium Au-197(n,γ)Au-198 reaction rate and the S-32(n,p)P-32, In-115(n,n')In-115m, Rh-103(n,n')Rh-103m and Al-27(n,α)Na-24 threshold reaction rates. Penetration measurements were made along the nuclear centre line, which is the horizontal axis of the system passing through the centre of the fission plate. Lateral distributions were also measured at various positions in the shields, the foils being located at intervals of 25 cm up and down from the nuclear centre line. The labelling convention for the measurement locations is given in Figure 2.

A fraction of the neutrons present in the experimental array originates from leakage from the NESTOR core. To obtain a true comparison between measurement and a calculation using the fission plate source, the NESTOR core component must be subtracted from the measurement. There are two methods by which the background component can be estimated.

The best method is to repeat the measurement with the fissile content of the fission plate removed, i.e. an unfuelled measurement. This is a time consuming method as measurements have to be made twice at every point, once with the fuel and once without. The combination of low fluxes and low sensitivities of integral detectors can make foreground fuelled measurements difficult at deep penetration with the result that unfuelled measurements become impossible.

Background corrections of acceptable accuracy can be made for the high energy threshold reactions by a second method using the hydrogen filled proportional counters of the TNS system /12/ in integral mode. Here measurements of the neutron count-rates in the shield with the ASPIS shutter open and closed are required together with a measure of the shut-down ratio of the fission plate when the neutron shutter is closed. This technique has been used for determining the background correction for the proportional counters; the correction was found to be around 2% throughout the shield and a value of 2% is recommended for the four threshold detectors at all positions in the shield.

The unfuelled technique for background correction has been adopted for the gold measurements as there is a significant component of the low energy flux which does not arise from the fission plate particularly near the fission plate itself where the fuelled to unfuelled ratio can be as low as 3.

The reaction effective threshold energies for the Rh-103(n,n'), In-115(n,n'), S-32(n,p) and Al-27(n,α) dosimeters, in a U-235 fission neutron spectrum similar to that of the Iron-88 experiment, are respectively 0.69 MeV, 1.30 MeV, 2.8 MeV and 7.30 MeV (see /13/). Nevertheless, since the effective energy threshold is not a completely satisfactory parameter for the characterization of the energy dependent cross section functions, the reported values give only a rough indication of the start of the response for the specific dosimeter. If one wishes to characterize the dosimeter response energy range more accurately, the energy range corresponding to 90% of the response and the median energy of the response should be taken into account. The median energy is defined such that, in the specific spectrum, the responses

below and above this energy numerical value are equal. Secondly, the definition of the energy range corresponding to 90% of the total response of a dosimeter implies that 5% of the response is below the lower boundary and 5% above the upper boundary of this energy range. A synthesis of these data, taken from reference /13/, for the four dosimeters used in the Iron-88 experiment is reported in Table 3 to give more specific detailed information addressed to obtain a more precise analysis in the comparison of the experimental and calculated dosimetric results.
In practice the experimental results coming from Rh-103(n,n') and In-115(n,n') (see /14/) correspond to neutron fluxes above about 1.0 MeV and the experimental results from S-32(n,p) with neutron fluxes above about 3.0 MeV.

Table 3

Iron-88 - Threshold Activation Dosimeter Parameters in a U-235 Fission Neutron Spectrum.

Dosimeter	Effective Energy Threshold [MeV]	90% Response Energy Range [MeV]	Median Energy [MeV]
Rh-103(n,n')	0.69	0.72 – 5.8	2.3
In-115(n,n')	1.30	1.1 – 5.9	2.6
S-32(n,p)	2.80	2.3 – 7.3	4.0
Al-27(n,α)	7.30	6.4 – 12.0	8.6

Figure 2 Measurement locations for the iron 88 single material benchmark experiment

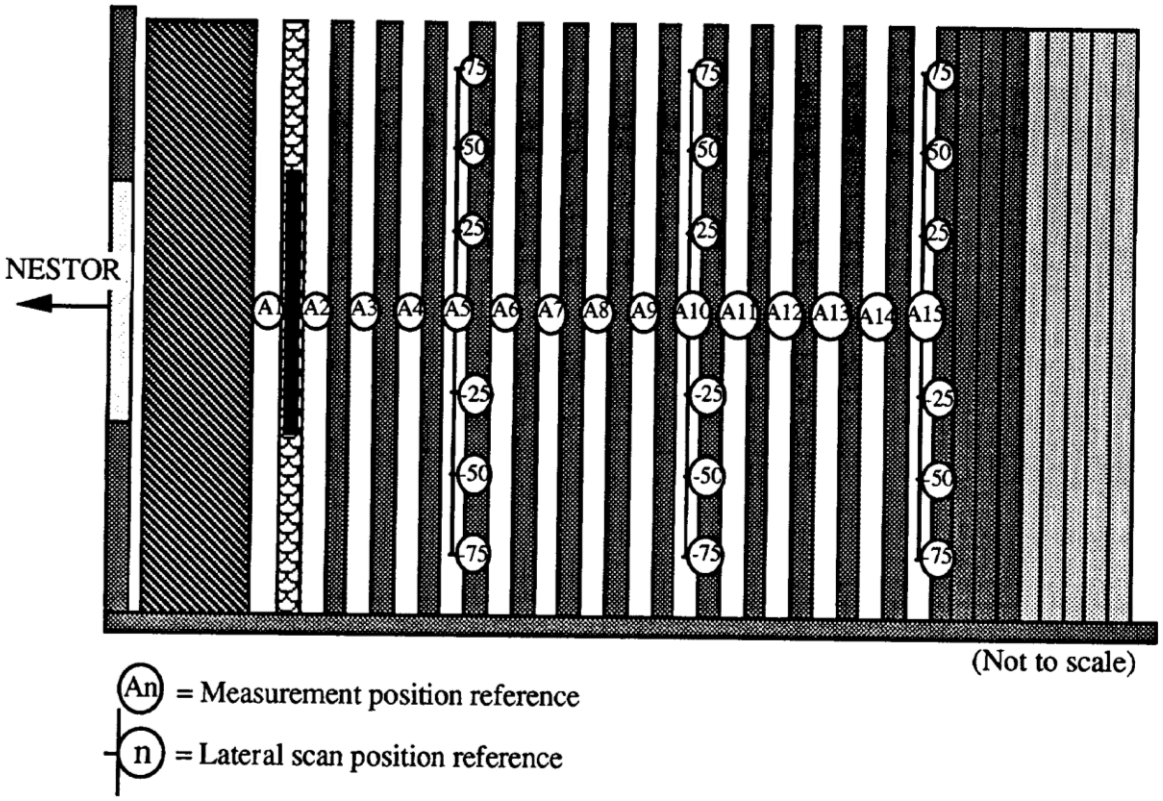

Penetration measurements are located on the nuclear centre line as defined below

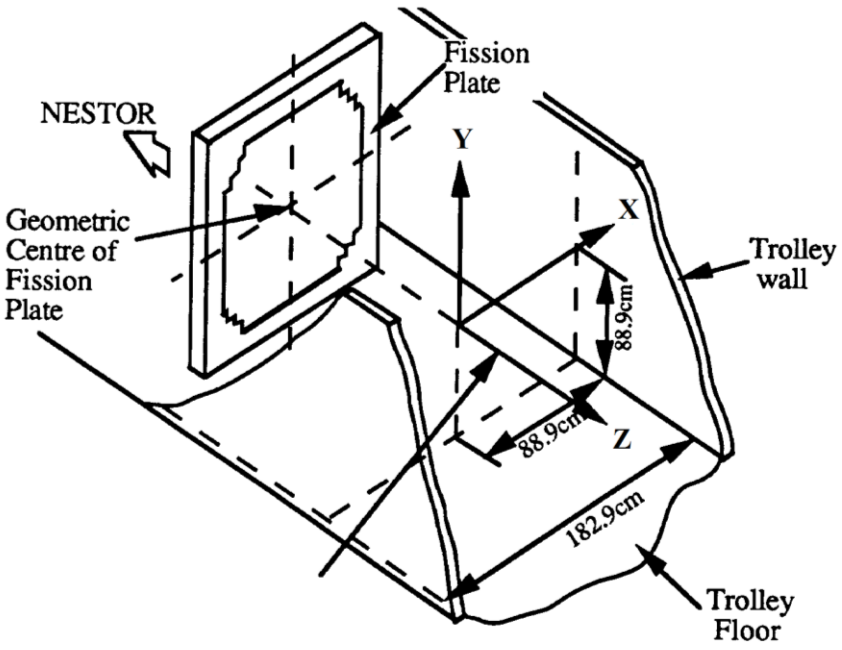

2.4 - Source Description

A schematic diagram of the fission plate is shown in Figure 3. It comprises an aluminium frame which fills the height and width of the ASPIS trolley. Located within the frame are 13 separate fuel elements. A schematic view of an individual fuel element is shown in Figure 4. Each element has two 12 mm thick aluminium cover plates which attach on either side of the top and bottom locating end pieces leaving a 5 mm separation in which U/Al alloy fuel strips are located. The fuel strips are 80% by weight aluminium and 20% by weight of uranium enriched to 93% having a density of 3.256 g/cm^3. Each strip is nominally 30.5 mm wide and 1 mm thick and is fixed to the rear cover plate by M5 screws.

Three columns of fuel strips laid side by side fill the width of the element. There is depth for 4 fuel strips within each element leaving a 1 mm clearance gap next to the front cover plate. In the current configuration only the central two strips in each column contain U/Al alloy, the outer two are both blanks manufactured from aluminium. To approximate to a disc fission neutron source the axial fuel loading within each element has been arranged to the specification shown in Figure 5 by the substitution of aluminium blanks for fuel where necessary giving 4 mm of aluminium in the unfuelled regions.

The position of the fission plate is shown in Figure 2. The centre of the fuel is at a height of 889 mm from the floor of the trolley and at 889 mm from the right hand wall of the trolley when looking towards the NESTOR core. The measurements were made on this Z horizontal nuclear axis passing through the centre of the fission plate.

The approach taken to obtain the absolute power distribution within the fission plate is summarised as follows:

1. Mn-55(n,γ)Mn-56 reaction-rates are measured over the front surface of the fission plate to define a thermal flux profile in X and Y.

2. The distribution of the U-235 content within the fuel is assessed.

3. 1. and 2. are combined to provide a relative fission-rate profile in X and Y.

4. The relative fission profile in the Z direction through the fuel is obtained from absolute measurements of fission-rate in the plate as described below.

5. The fission-rate profile is normalised to absolute measurements of the fission-rate per NESTOR Watt in the plate which are made by counting fission product decay rates in samples taken from the central strip of the central element at the centre, bottom and halfway between the centre and bottom of the fuel.

6. The neutron source distribution is obtained from the absolute fission-rate distribution.

The manganese reaction-rate measurements on the front face of the plate were input to the CRISP code /15/ to define the manganese reaction-rate surface covering the plate. From this surface the average manganese reaction-rate within the elements of any source mesh overlaid onto the fission plate can be defined. The fission-rate profile in X and Y is taken as the

manganese reaction-rate profile on the front face of the fuel plate. This has been normalised to give a plate power of 1 Watt and the resulting neutron source distribution is shown in Table 4. Constants of 3.121E+10 fissions per Watt and 2.437 neutrons per fission have been used in this derivation.

The absolute fission rate in the fuel was found to be between 5% and 16% higher in the strip nearer to NESTOR. This difference is caused by the attenuation of thermal neutrons from NESTOR through the 1 mm fuel strips. However, the attenuation of the neutrons produced by fission is small over this distance so an assumption of no Z dependence in the source strength has been made.

The absolute power in the fission plate, expressed as plate Watts per NESTOR Watt, has been determined by combining measurements of the absolute fission-rate at spot values, gained by fission product decay line counting, with the fission-rate profile data derived in CRISP. The analysis is rather involved and the result was an absolute plate power of 5.68E-04 Watts per NESTOR Watt. The uncertainty on the plate power is 8% at the two standard deviations (2σ) level.

Table 4

Source Distribution on the Fission Plate.

0	0	0	0	0	0	2.973	2.994	2.865	0	0	0	0	0	0
0	0	0	0	0	3.173	3.496	3.537	3.404	2.975	0	0	0	0	0
0	0	0	0	3.176	3.711	4.088	4.149	4.015	3.529	2.890	0	0	0	0
0	0	0	3.186	3.500	4.092	4.514	4.587	4.446	3.925	3.240	2.886	0	0	0
0	0	3.249	3.635	3.999	4.696	5.197	5.286	5.130	4.555	3.807	3.422	3.009	0	0
0	3.150	3.575	4.003	4.412	5.202	5.770	5.870	5.699	5.080	4.282	3.873	3.431	2.970	0
3.040	3.322	3.769	4.223	4.660	5.505	6.110	6.215	6.034	5.387	4.559	4.133	3.673	3.188	2.850
3.132	3.427	3.893	4.364	4.815	5.684	6.304	6.412	6.227	5.563	4.710	4.270	3.792	3.287	2.932
3.026	3.325	3.784	4.239	4.669	5.491	6.079	6.183	6.009	5.364	4.523	4.084	3.607	3.103	2.751
0	3.136	3.574	4.001	4.400	5.157	5.701	5.802	5.643	5.031	4.221	3.795	3.331	2.843	0
0	0	3.182	3.562	3.912	4.572	5.053	5.149	5.013	4.461	3.713	3.317	2.887	0	0
0	0	0	3.004	3.299	3.855	4.267	4.357	4.247	3.766	3.101	2.748	0	0	0
0	0	0	0	2.896	3.396	3.770	3.855	3.758	3.320	2.712	0	0	0	0
0	0	0	0	0	2.745	3.072	3.150	3.067	2.685	0	0	0	0	0
0	0	0	0	0	0	2.458	2.525	2.448	0	0	0	0	0	0

Units are neutrons × cm^{-3} × $second^{-1}$ × 1.0E+07.
The plate power for this distribution is 1 Watt.

Coordinate boundaries for source distribution.
Units are cm.

X	-52.25	-49.08	-45.92	-39.58	-36.42	-30.08	-14.25	-4.75
	4.75	14.25	30.08	36.42	39.58	45.92	49.08	52.25
Y	-51.44	-47.63	-40.64	-35.56	-31.75	-19.69	-15.88	-5.29
	5.29	15.88	19.69	31.75	35.56	40.64	47.63	51.44

Figure 3 Schematic diagram of fission plate

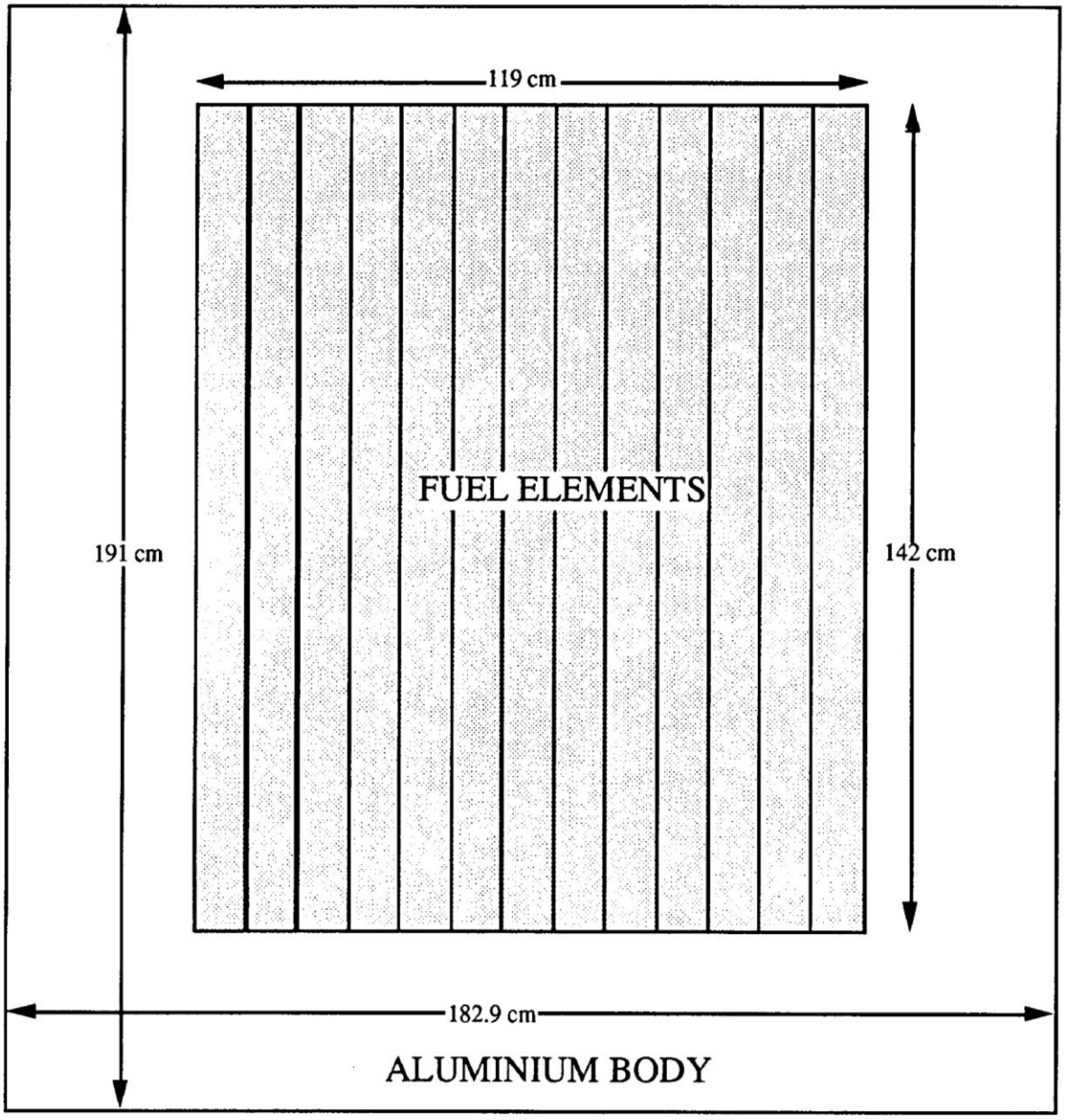

Figure 4 Diagram of fuel element

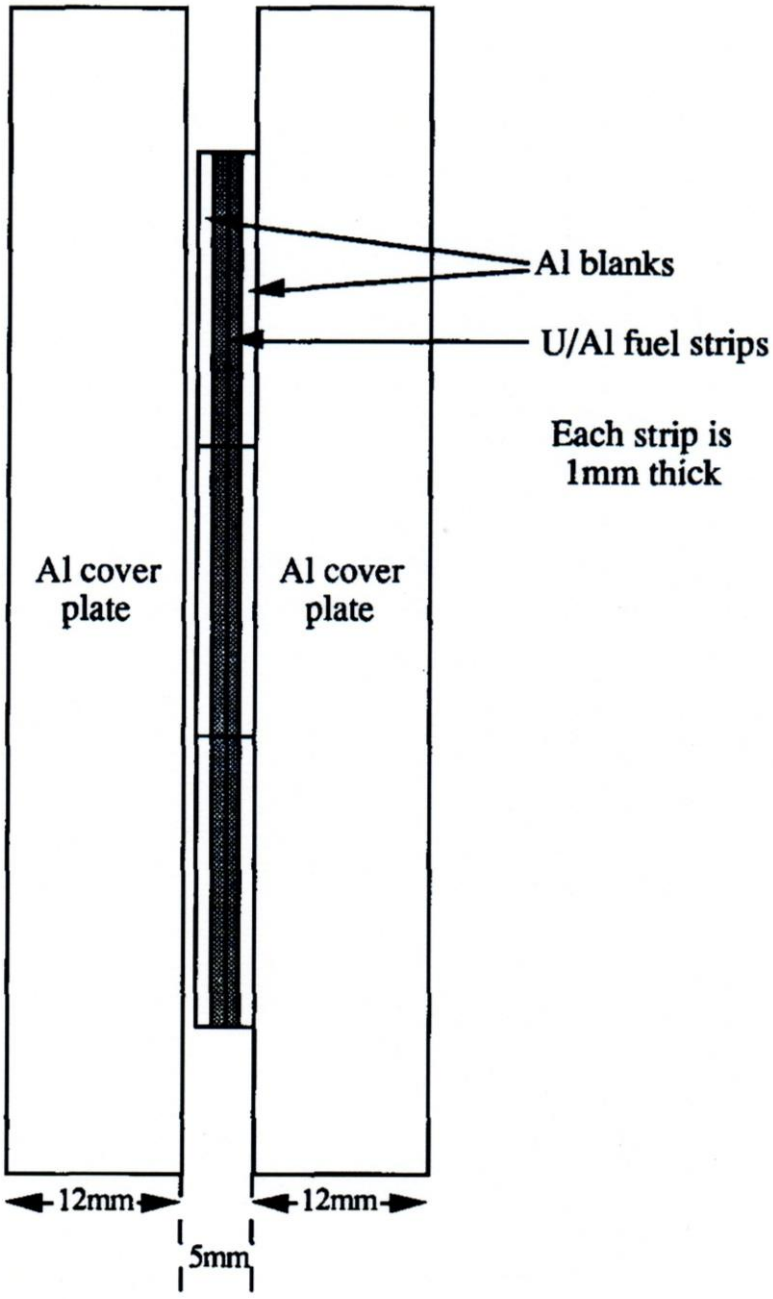

Figure 5 Disposition of fuel in fission plate

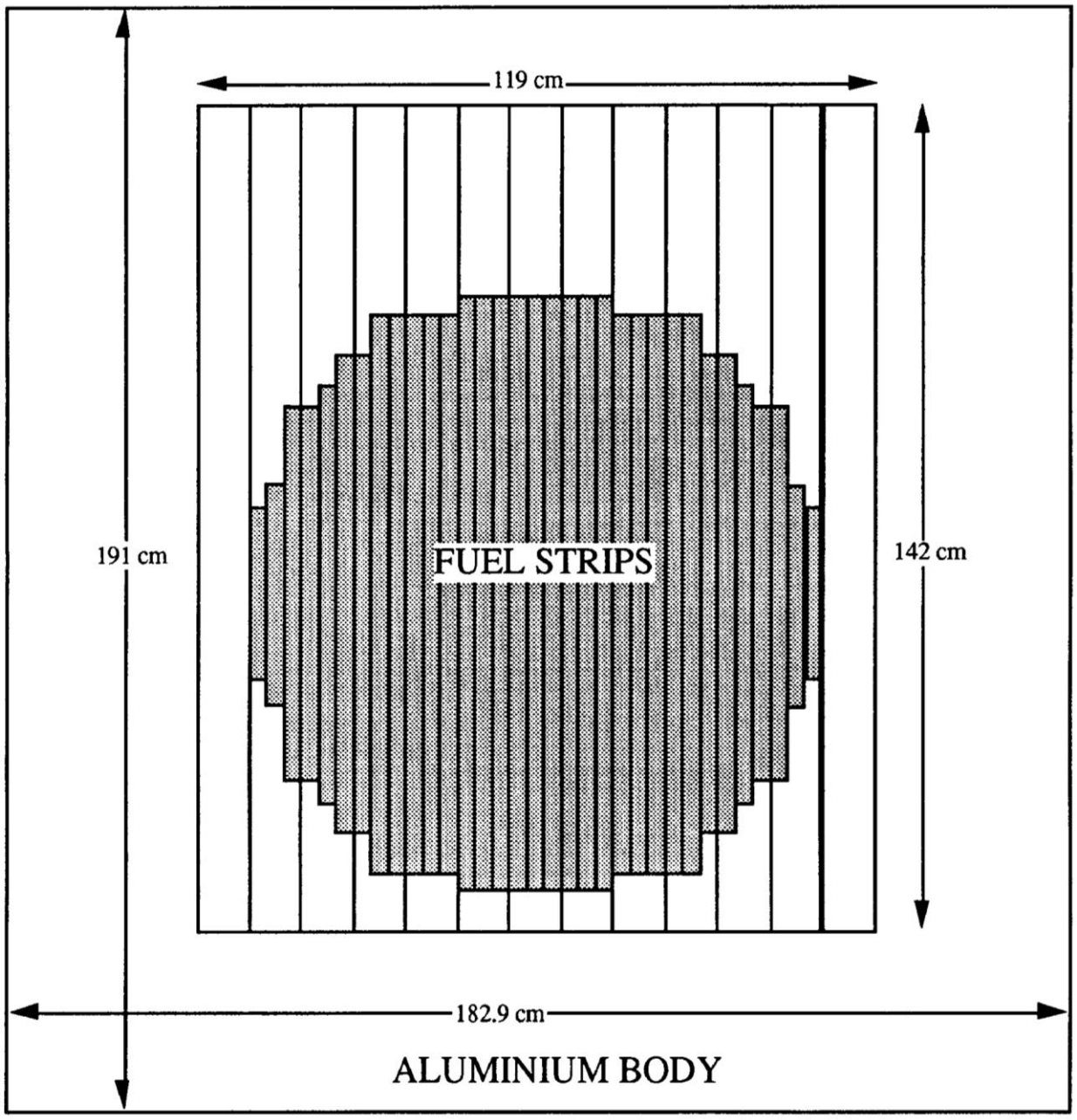

Figure 6

Section Normal to the Z Horizontal Axis at the Fission Plate Centre.

Position of the Fission Plate with respect to the ASPIS Trolley.

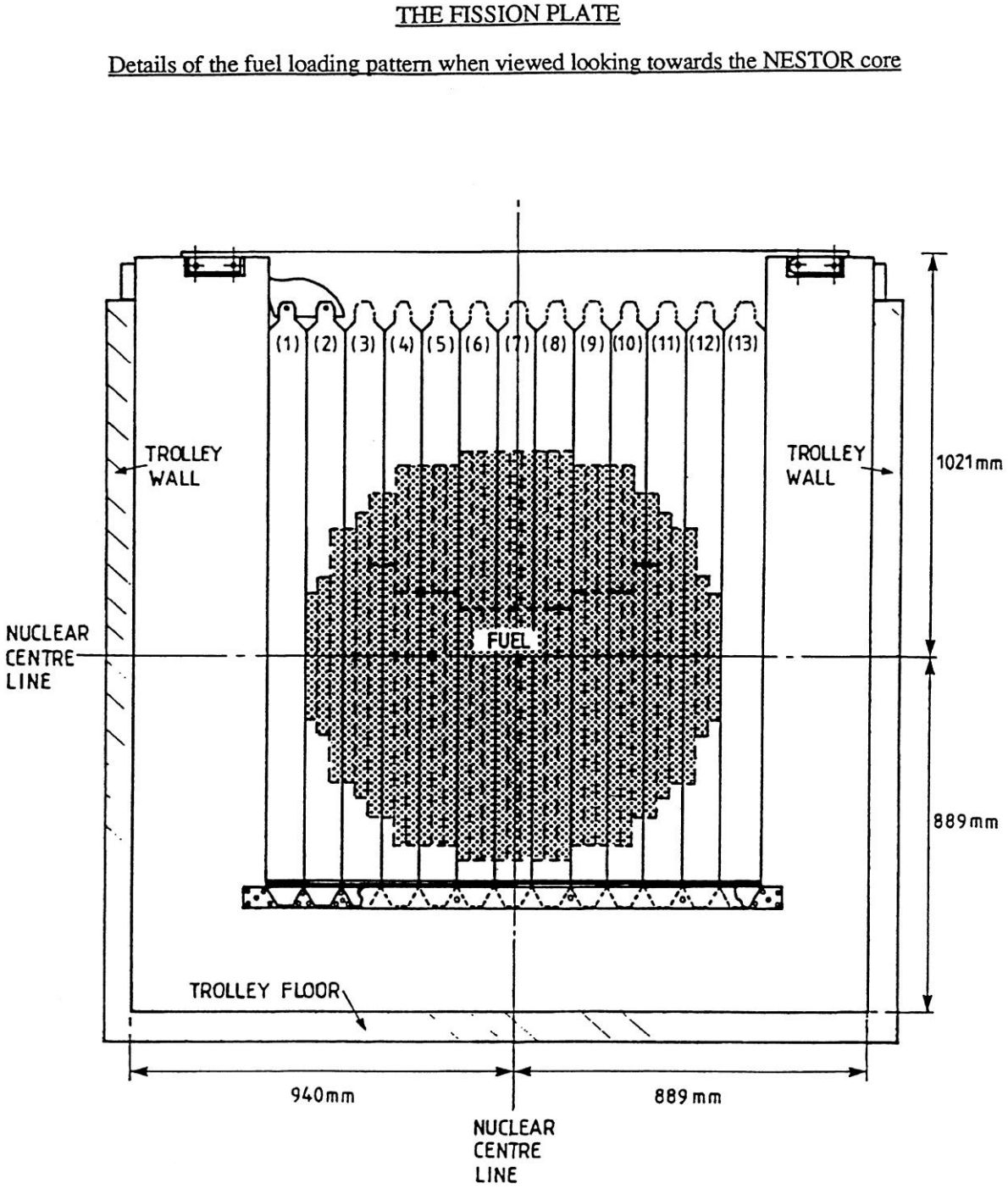

3.0 - TRANSPORT CALCULATIONS

3.1 - The BUGJEFF311.BOLIB Library

The ENEA-Bologna BUGJEFF311.BOLIB /1/ is a broad-group coupled neutron/photon working cross section library in FIDO-ANISN /7/ format with parameterized cross section sets of problem-dependent self-shielded neutron cross sections, dedicated to the previously cited LWR radiation shielding and radiation damage applications and, in particular, to the RPV dosimetry analyses. The BUGJEFF311.BOLIB library adopts (see Tables 5 and 6) the neutron and photon energy group structures (47 neutron groups + 20 photon groups) of the similar ORNL BUGLE-96 /10/ broad-group working library in FIDO-ANISN format, derived from the ORNL VITAMIN-B6 /10/ library in AMPX format based on the ENDF/B-VI.3 /16/ evaluated data library and specifically conceived for the same previously cited applications in LWRs. BUGJEFF311.BOLIB is the first BUGLE-type multi-group library, based on OECD-NEADB JEFF nuclear data, freely released by OECD-NEADB and ORNL-RSICC at international level.

BUGJEFF311.BOLIB was obtained through problem-dependent cross section collapsing from the ENEA-Bologna VITJEFF311.BOLIB /17/ fine-group coupled neutron/photon cross section library for nuclear fission applications, based on the JEFF-3.1.1 /8/ (see also /9/) evaluated nuclear data library and on the Bondarenko /18/ (f-factor) method for the treatment of neutron resonance self-shielding and temperature effects. The VITJEFF311.BOLIB library is a “pseudo-problem-independent” library in AMPX format, i.e., a fine-group library prepared with enough detail in energy, temperatures and neutron resonance self-shielding so as to be applicable to a wide range of physical systems. VITJEFF311.BOLIB is characterized in particular by the same neutron and photon energy group structures (199 neutron groups + 42 photon groups) as VITAMIN-B6.

Concerning the BUGJEFF311.BOLIB library validation on integral neutron shielding benchmark experiments, a limited preliminary testing was successfully performed with the 3D TORT-3.2 discrete ordinates transport code on the PCA-Replica 12/13 /19/ /20/ (Winfrith, UK) and VENUS-3 /21/ (Mol, Belgium) engineering neutron shielding benchmark integral experiments, whose compositional and geometrical specifications were taken from the fission reactor shielding section of the ORNL-RSICC/OECD-NEA Data Bank SINBAD REACTOR /3/ international database of shielding benchmark experiments.
The two cited engineering integral neutron shielding benchmark experiments are specifically dedicated to test the accuracy of nuclear data and transport codes employed, in particular, in the PWR shielding and pressure vessel dosimetry.

The PCA-Replica 12/13 low-flux engineering neutron shielding benchmark experiment is a water/iron benchmark experiment including PWR thermal shield and pressure vessel simulators. The source of neutrons was a thin fission plate of highly enriched uranium (93.0 w% in U-235), irradiated by the NESTOR low-power experimental reactor through a graphite thermal column (total thickness 43.91 cm). Beyond the fission plate, the PCA-Replica shielding array (12/13 experimental configuration with two water gaps of about 12 cm and 13 cm) was arranged in a large parallelepiped steel tank filled with water. After a first water gap (12.1 cm), there was the stainless steel thermal shield simulator (5.9 cm), the second water gap (12.7 cm), the mild steel pressure vessel simulator (thickness T = 22.5 cm) and a wide

box made of a thin layer of aluminium simulating the air cavity between the pressure vessel and the biological shield in a real PWR.

The VENUS-3 low-flux engineering neutron shielding benchmark experiment is closely related to PWR pressure vessel (PV) safety. It was designed to test the accuracy of the nuclear data and transport codes in the calculation of the neutron radiation damage parameters in stainless steel reactor components, in a context of great precision of the experimental results. Among the available experiments, the VENUS-3 configuration offers the exceptional advantage of exhibiting a realistic radial core shape and a typical PWR neutron spectrum. Typical "17x17" PWR fuel assemblies were employed and a mock-up of the pressure vessel internals, representative of a three-loop Westinghouse power plant, was prepared. VENUS-3 was conceived taking into account that, for some early built reactors, it was proposed to reduce the lead factor at the level of the PV horizontal welding by loading Partial Length Shielded Assemblies (PLSA) at the most critical corners of the core periphery (the shielded part was obtained by replacing part of the fuel length by a stainless steel rod). VENUS-3 was addressed to test this improvement, introducing a PLSA region in the core, and to permit the validation of the analytical methods needed to predict the azimuthal variation of the fluence in the pressure vessel. The core has a cruciform-shaped configuration. The core consisted of three types of fuel pins: 1) stainless-steel-clad UO_2 rods (typical of a "15x15" lattice of the early Generation I reactors of Westinghouse plants) containing 4% enriched U-235, 2) zircaloy-clad UO_2 rods containing 3.3% enriched U-235 and 3) zircaloy-clad UO_2 rods containing 3.3% enriched U-235 over the upper half of their height and zircaloy-clad steel rods over the lower half. The first two types of fuel pins were of uniform composition over their complete height. The 4% enriched rods were positioned in the inner part of the core while the 3.3% enriched rods were located in the arms of the cross configuration together with the PLSA-modified rods.

Starting from the centre, the core quadrant between 0° and 90° may be divided in the following 10 horizontal radial regions:

- the CENTRAL HOLE (water);
- the INNER BAFFLE (stainless steel thickness: 2.858 cm);
- the 4/0 FUEL REGION: 4% enriched uranium fuel rods and 11 pyrex control rods, typical of PWR poison clusters;
- the 3/0 FUEL REGION: 3.3% enriched uranium fuel rods and PLSA rods;
- the OUTER BAFFLE (stainless steel thickness. 2.858 cm);
- the REFLECTOR (water minimum thickness: 2.169 cm);
- the BARREL (stainless steel thickness: 4.99 cm);
- the WATER GAP (water thickness: 5.80 cm);
- the NEUTRON PAD (stainless steel average thickness: 6.72 cm);
- the VENUS environment, i.e., the jacket (air filled), the reactor vessel (stainless steel) and the reactor room (air).

In the present program of cross section testing activities it was decided to add another important neutron shielding benchmark experiment, dedicated to the validation of BUGJEFF311.BOLIB. In particular BUGJEFF311.BOLIB was used in three-dimensional transport analyses dedicated to a single-material (iron) benchmark experiment named Iron-88

/2/. This experiment permits to verify the neutron deep penetration (about six decades of neutron flux attenuation) through a mild steel layer of about 67 cm and is complementary with respect to the two previously cited engineering benchmark shielding experiments. It is underlined that the performance of the iron nuclear data are obviously essential for any fission reactor applications. It is well known in fact that the LWR pressure vessels and the so-called internals are made of different types of steels where in any case the iron cross sections, and in particular those of Fe-56, with an isotopic abundance of about 92% in natural iron, play a crucial role in the accurate prediction of the EoL (End-of-Life) neutron fluence.

Table 5

Neutron Group Energy and Lethargy Boundaries for the BUGJEFF311.BOLIB Library.

Group	Upper Energy [eV]	Upper Lethargy
1	1.7332E+07	-5.4997E-01
2	1.4191E+07	-3.5002E-01
3	1.2214E+07	-2.0000E-01
4	1.0000E+07	0.
5	8.6071E+06	1.5000E-01
6	7.4082E+06	3.0000E-01
7	6.0653E+06	5.0000E-01
8	4.9659E+06	7.0000E-01
9	3.6788E+06	1.0000E-00
10	3.0119E+06	1.2000E+00
11	2.7253E+06	1.3000E+00
12	2.4660E+06	1.4000E+00
13	2.3653E+06	1.4417E+00
14	2.3457E+06	1.4500E+00
15	2.2313E+06	1.5000E+00
16	1.9205E+06	1.6500E+00
17	1.6530E+06	1.8000E+00
18	1.3534E+06	2.0000E+00
19	1.0026E+06	2.3000E+00
20	8.2085E+05	2.5000E+00
21	7.4274E+05	2.6000E+00
22	6.0810E+05	2.8000E+00
23	4.9787E+05	3.0000E+00
24	3.6883E+05	3.3000E+00
25	2.9721E+05	3.5159E+00
26	1.8316E+05	4.0000E+00
27	1.1109E+05	4.5000E+00
28	6.7379E+04	5.0000E+00
29	4.0868E+04	5.5000E+00
30	3.1828E+04	5.7500E+00
31	2.6058E+04	5.9500E+00
32	2.4176E+04	6.0250E+00
33	2.1875E+04	6.1250E+00
34	1.5034E+04	6.5000E+00
35	7.1017E+03	7.2500E+00
36	3.3546E+03	8.0000E+00
37	1.5846E+03	8.7500E+00
38	4.5400E+02	1.0000E+01
39	2.1445E+02	1.0750E+01
40	1.0130E+02	1.1500E+01
41	3.7266E+01	1.2500E+01
42	1.0677E+01	1.3750E+01
43	5.0435E+00	1.4500E+01
44	1.8554E+00	1.5500E+01
45	8.7643E-01	1.6250E+01
46	4.1399E-01	1.7000E+01
47	1.0000E-01	1.8421E+01
	1.0000E-05	2.7631E+01

Table 6

Photon Group Energy Boundaries for the BUGJEFF311.BOLIB Library.

Group	Upper Energy [eV]
1	1.4000E+07
2	1.0000E+07
3	8.0000E+06
4	7.0000E+06
5	6.0000E+06
6	5.0000E+06
7	4.0000E+06
8	3.0000E+06
9	2.0000E+06
10	1.5000E+06
11	1.0000E+06
12	8.0000E+05
13	7.0000E+05
14	6.0000E+05
15	4.0000E+05
16	2.0000E+05
17	1.0000E+05
18	6.0000E+04
19	3.0000E+04
20	2.0000E+04
	1.0000E+04

3.2 - Transport Calculation General Features

Fixed source transport calculations in Cartesian geometry were performed for the Iron-88 neutron shielding benchmark experiment using the ORNL TORT-3.2 /5/ three-dimensional discrete ordinates (S_N) code included in the ORNL DOORS-3.2 /22/ system of deterministic transport codes. The whole Iron-88 experimental array (see /2/ and 2.2) was reproduced with the TORT-3.2 code using the realistic inhomogeneous fission neutron source (see 2.4 and Table 4) emitted by the fission plate.

The TORT-3.2 code was used on a personal computer (CPU: INTEL PENTIUM D 3.40 GHz, 3.10 GB of RAM) under Linux openSUSE 10.2 (i586) operating system with FORTRAN-77 compiler g77, version 3.3.5-38.

The automatic generation of the spatial mesh grid and the graphical verification of the Iron-88 benchmark experiment geometrical model for TORT-3.2 were performed through the ENEA-Bologna BOT3P-5.3 /23/ (see also /24/, /25/ and /26/) pre/post-processor system.

The reference system adopted in the present calculations has its origin on the Z horizontal axis passing through the centre of the fission plate (see Figures 2 and 6) and normal to it. It is underlined that the centre of the fission plate is not aligned with the centre of the trolley face. In fact the centre of the trolley face is shifted by -2.55 cm in the X horizontal axis direction and by +6.6 cm in the Y vertical axis direction.

In all the calculations it was reproduced the whole three-dimensional Iron-88 experimental array in the (X,Y,Z) Cartesian geometry in order to assure a proper detailed description (see Figure 7) of the spatial inhomogeneity of the neutron source (see Table 4) emitted by the fission plate. In particular it was described a parallelepiped geometry with a 69X×86Y×278Z fine spatial mesh grid, where Z was the horizontal nuclear axis (see Figure 2) where the dosimetric measurement positions were located. Volumetric meshes with sides always inferior to 1.0 cm were described along the Z axis, in correspondence of the measurement region, to obtain the best accuracy in the calculation results. In the measurement positions along the Z axis, i.e. in the 0.74 cm air gaps between each mild steel slab component, volumetric meshes with sides along the Z axis always inferior to 0.25 cm were described.

The horizontal section (at the vertical axis position Y = 0.0 cm) of the Iron-88 compositional and geometrical model, reproduced in all the TORT-3.2 (X,Y,Z) calculations, is reported in Figure 8 together with the dosimeter locations (×). A detail of the Figure 8 is represented in the Figure 9, representing an enlargement of the compositional and geometrical model in the measurement region where it is possible to see better the 0.74 cm air gaps, between the various mild steel slab components, and the related dosimeter measurement locations.

The mild steel floor, roof and lateral walls of the trolley 1.91 cm thick (see 2.2) were simulated in the TORT calculations since they were originally represented in the input data of the Monte Carlo MCBEND /27/ code calculation example, reported in the Iron-88 benchmark experiment section of reference /3/.

The calculation model adopted includes a 1 m long graphite region (see Figure 8) to represent the region of the NESTOR reactor behind the trolley face and the fission plate (i.e. towards

NESTOR reactor from the fission plate), not contained in Table 1, where only the regions behind the fission plate up to the end of the trolley are indicated. As confirmed in the Iron-88 /2/ report at page 4, the realistic presence of the graphite zone will permit to obtain more accurate Au-197(n,γ)Au-198 calculated reaction rate results, for the moment not available in the present analysis, particularly in the first five measurement positions (see Figure 2). Concerning this, it was decided to introduce the previously cited additional graphite region in all the present and future calculations (producing in particular the gold reaction rate results) to compare all the reaction rate results in a consistent way.

The ENEA-Bologna ADEFTA-4.1 /28/ program was employed in the calculation of the atomic densities of the isotopes involved in the compositional model on the basis of the atomic abundances reported in the BNL-NNDC database /29/ included in ADEFTA. The Iron-88 atomic densities were calculated using the densities and the weight fractions reported in the Table 2 of the Iron-88 /2/ report.

The ENEA-Bologna BUGJEFF311.BOLIB /1/ (JEFF-3.1.1 /8/ /9/ data) working library was used in the transport calculations with TORT-3.2, in alternative to the ORNL BUGLE-96 /10/ (ENDF/B-VI.3 /16/ data) similar working library considered a well tested reference library.

All the calculations were performed only with the first 29 neutron groups (see Table 5), above 3.1828E+04 eV, since all the neutron energy thresholds of the four employed dosimeters are above this neutron energy value.

Both infinite dilution and self-shielded neutron cross sections were selected. Proper self-shielded cross sections from the BUGJEFF311.BOLIB and BUGLE-96 library packages were used when available. In particular it is underlined that the mild steel and stainless steel regions of Iron-88 are characterized by atomic densities quite similar to those used to calculate the background cross sections, employed in the self-shielding of the BUGJEFF311.BOLIB and BUGLE-96 neutron cross sections. Group-organized files of macroscopic cross sections, requested by TORT-3.2 and derived from the BUGJEFF311.BOLIB and BUGLE-96 working libraries in FIDO-ANISN format, were prepared through the ORNL GIP (see /15/) program, specifically dedicated to the discrete ordinates transport codes (ANISN-ORNL, DORT, TORT) of the DOORS system. The ENEA-Bologna ADEFTA-4.1 program was used not only to calculate the atomic densities for the benchmark experiment compositional model but also to handle them properly in order to automatically prepare the macroscopic cross section sets of the compositional model material mixtures in the format required by GIP.

Fixed source transport calculations with one source (outer) iteration and 60 inner iterations were performed using fully symmetrical discrete ordinates directional quadrature sets for the flux solution. The P_3-S_8 approximation was adopted as the standard reference in all the calculations with the BUGJEFF311.BOLIB and BUGLE-96 libraries. P_N corresponds to the order of the expansion in Legendre polynomials of the scattering cross section matrix and S_N represents the order of the flux angular discretization. It is underlined that the P_3-S_8 approximation is the most widely used option in the fixed source calculations dedicated to LWR safety analyses.

The theta-weighted difference approximation was selected for the flux extrapolation model.

In all the calculations the same numerical value (1.0E-03) for the point-wise flux convergence criterion was employed.
The vacuum boundary condition was selected at the left, right, inside, outside, bottom and top geometrical boundaries.

Concerning the Rh-103(n,n')Rh-103m, In-115(n,n')In-115m, S-32(n,p)P-32 and Al-27(n,α)Na-24 nuclear reaction cross sections for the four threshold activation dosimeters, used in the present Iron-88 transport analysis, they were derived (see /1/ and /30/) from the IAEA IRDF-2002 /6/ International Reactor Dosimetry File. The dosimeter cross sections for the BUGJEFF311.BOLIB calculations were obtained from IRDF-2002 using two neutron weighting spectra in the 199-group neutron energy structure, typical of the VITJEFF311.BOLIB and VITAMIN-B6 mother libraries: flat weighting and 1/4 T RPV weighting. As flat neutron weighting spectrum, the constant numerical value of unity was assumed in all the neutron groups. On the contrary, the 1/4 T RPV neutron weighting spectrum was obtained (see /1/ and /30/) through a one-dimensional transport calculation describing the in-vessel and ex-vessel radial geometry of a PWR, using the VITJEFF311.BOLIB /17/ fine-group mother library of BUGJEFF311.BOLIB, characterized by the previously mentioned 199-group neutron energy structure. In particular the 1/4 T RPV neutron weighting spectrum was calculated in a steel zone, the PWR RPV, at a spatial position corresponding to one quarter of the thickness (T) of the reactor pressure vessel (1/4 T RPV).

The nuclear reaction cross sections for the Rh-103(n,n')Rh-103m, In-115(n,n')In-115m, S-32(n,p)P-32 and Al-27(n,α)Na-24 neutron dosimeters were obtained in the 47-group neutron energy structure typical of the BUGJEFF311.BOLIB and BUGLE-96 libraries, through proper data processing using the IRDF-2002 data and the two previously cited 199-group neutron weighting spectra.
The nuclear reaction cross sections obtained with both flat and 1/4 T RPV weighting spectra were employed in all the calculations but, for this type of transport analysis dedicated to the Iron-88 (iron) single material neutron shielding benchmark experiment, the dosimeter cross sections obtained with the 1/4 T RPV weighting were considered more proper since this neutron weighting spectrum was obtained within a similar iron region.

Concerning the IRDF-2002 1/4 T RPV weighting dosimeter cross sections used in the transport calculations with BUGLE-96, they were obtained in ENEA-Bologna, for the present transport analysis, with the same calculation procedure previously described, using the 1/4 T RPV neutron weighting spectrum calculated at ORNL with the VITAMIN-B6 fine-group mother library of BUGLE-96.

It is underlined that, for the same specific dosimeter, the group numerical values of each flat weighting cross section set in the 47-group neutron energy structure, typical of the BUGJEFF311.BOLIB and BUGLE-96 libraries, are obviously identical in the transport calculations using BUGJEFF311.BOLIB and BUGLE-96. On the contrary, for the same specific dosimeter, the group numerical values of the 1/4 T RPV weighting cross section set, respectively used in the BUGJEFF311.BOLIB and BUGLE-96 calculations, are slightly different. In fact the 1/4 T RPV weighting dosimeter cross section sets, respectively used with BUGJEFF311.BOLIB and BUGLE-96, were obtained using separately two slightly different 199-group 1/4 T RPV neutron weighting spectra, respectively calculated with the

VITJEFF311.BOLIB and VITAMIN-B6 mother libraries, based respectively on JEFF-3.1.1 and ENDF/B-VI.3 different nuclear data.

The calculated reaction rates were obtained in all the experimental dosimeter positions in the 0.74 cm air gaps (see Figures 2, 7 and 8) between each mild steel slab component. The results for the Au-197(n, γ)Au-198 dosimeters, at present not yet available in the present work, will be obtained for the detailed final analysis of the Iron-88 benchmark experiment.

Finally, with respect to the fission neutron source normalization it was adopted the following approach. Taking into account that the fission plate neutron source is given in units of neutrons × cm^{-3} × $second^{-1}$ × 1.0E+07 (see Table 4), corresponding to 1 Watt of fission plate power, the "xnf" normalization factor in TORT-3.2 is given by:

$$xnf = 5.68E\text{-}04 \times 3.0E\text{+}04 \times 1.0E\text{-}24 = 1.704E\text{-}25$$

where

5.68E-04 (see /2/) are the fission plate Watts per NESTOR reactor Watt,

3.0E+04 Watts (see /2/) is the NESTOR reactor power and

1.0E-24 is a conversion factor taking into account that the atomic densities introduced in TORT-3.2 were expressed in atoms × $barn^{-1}$ × cm^{-1}.

Figure 7

Iron-88 - Vertical Section of the Fission Plate Neutron Source Distribution
Described in the TORT-3.2 (X,Y,X) Calculations.

Vertical Section at Z = 1.5 cm.
69X×86Y×278Z Spatial Meshes.

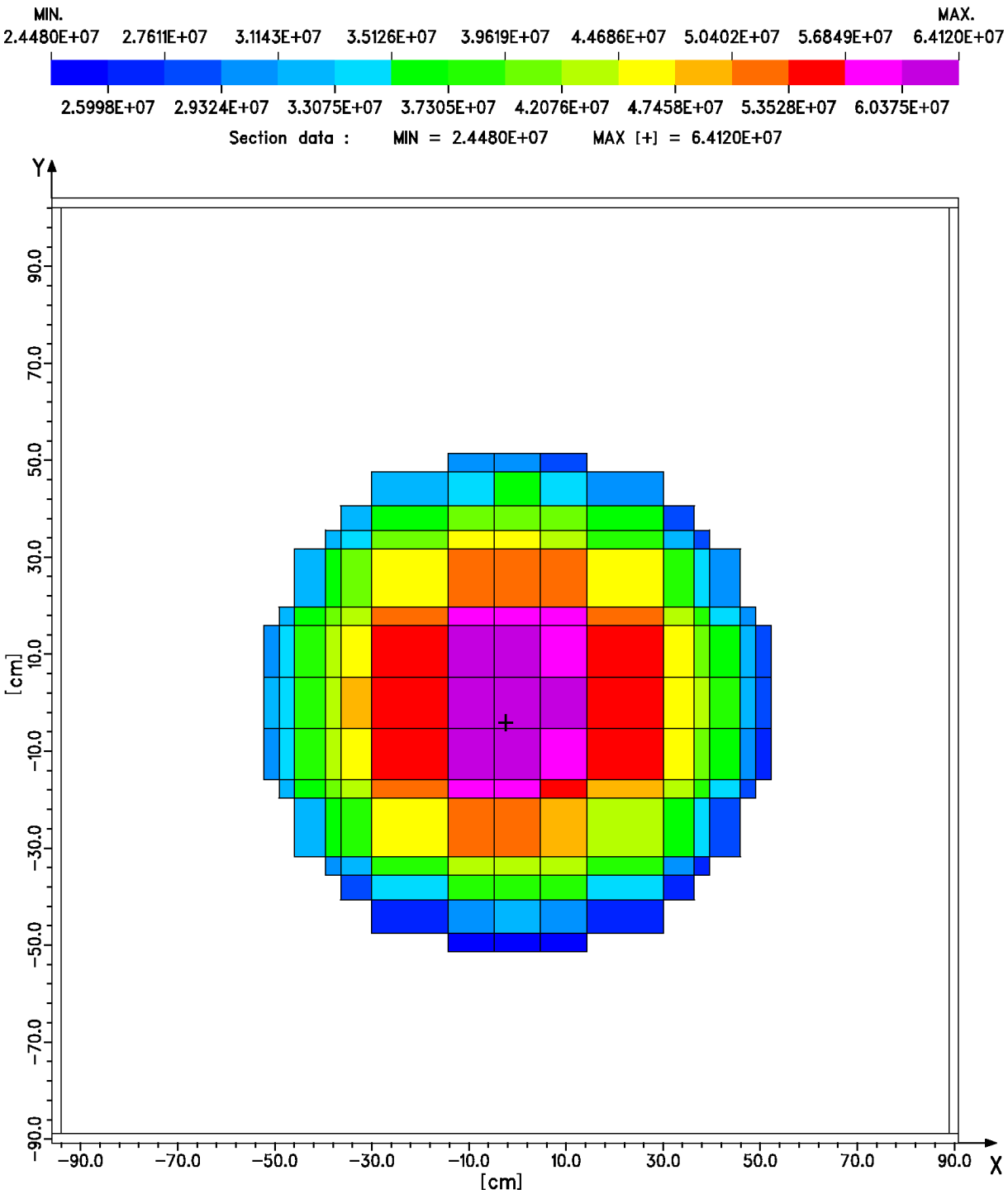

Figure 8

Iron-88 - Compositional and Geometrical Model in the TORT-3.2 (X,Y,Z) Calculations.

Horizontal Section at Y = 0.0 cm.
Dosimeter Locations "×", 69X×86Y×278Z Spatial Meshes.

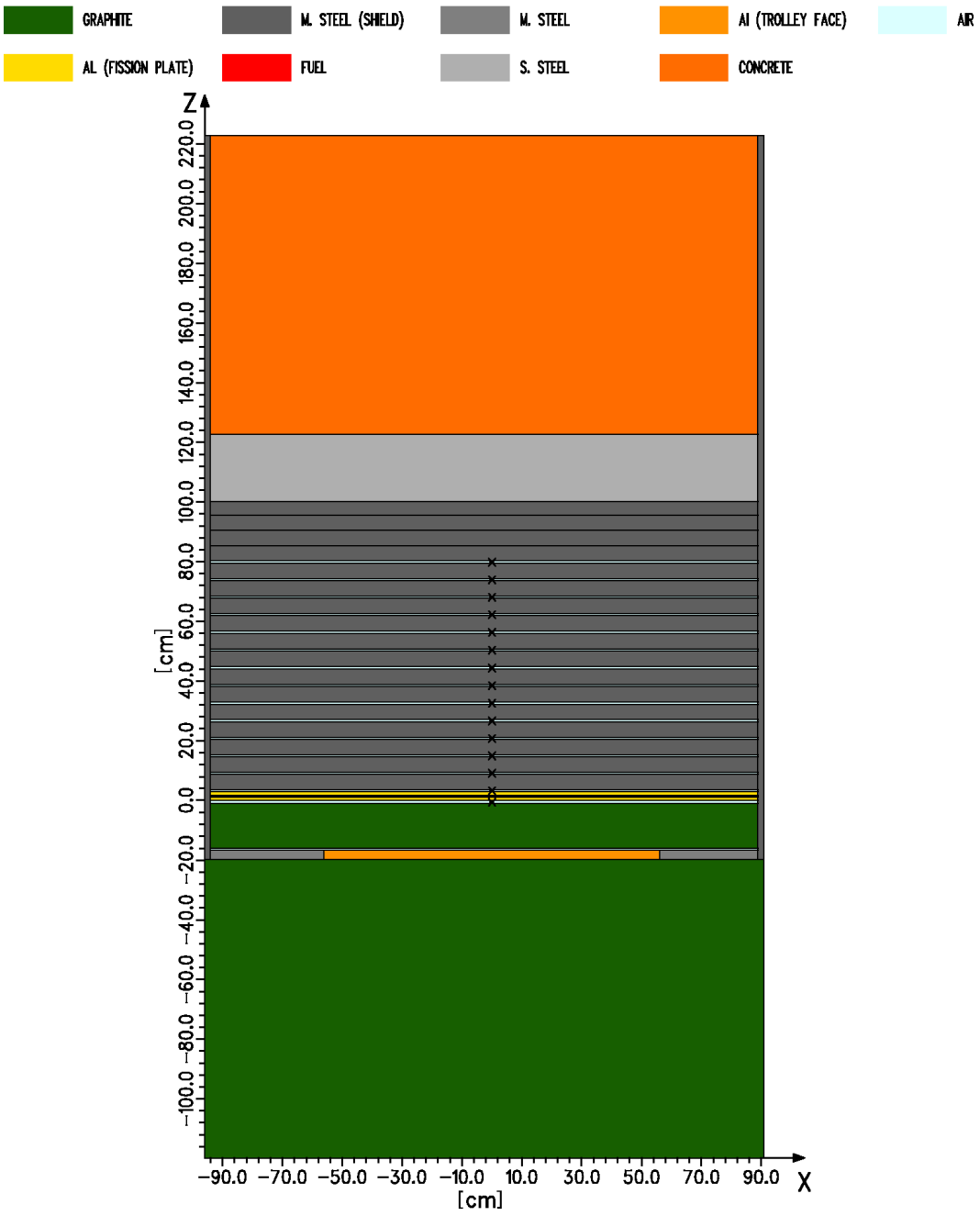

Figure 9

Iron-88 - Compositional and Geometrical Model in the TORT-3.2 (X,Y,Z) Calculations.

Enlargement of the Measurement Region, Horizontal Section at Y = 0.0 cm.
Dosimeter Locations "×", 69X×86Y×278Z Spatial Meshes.

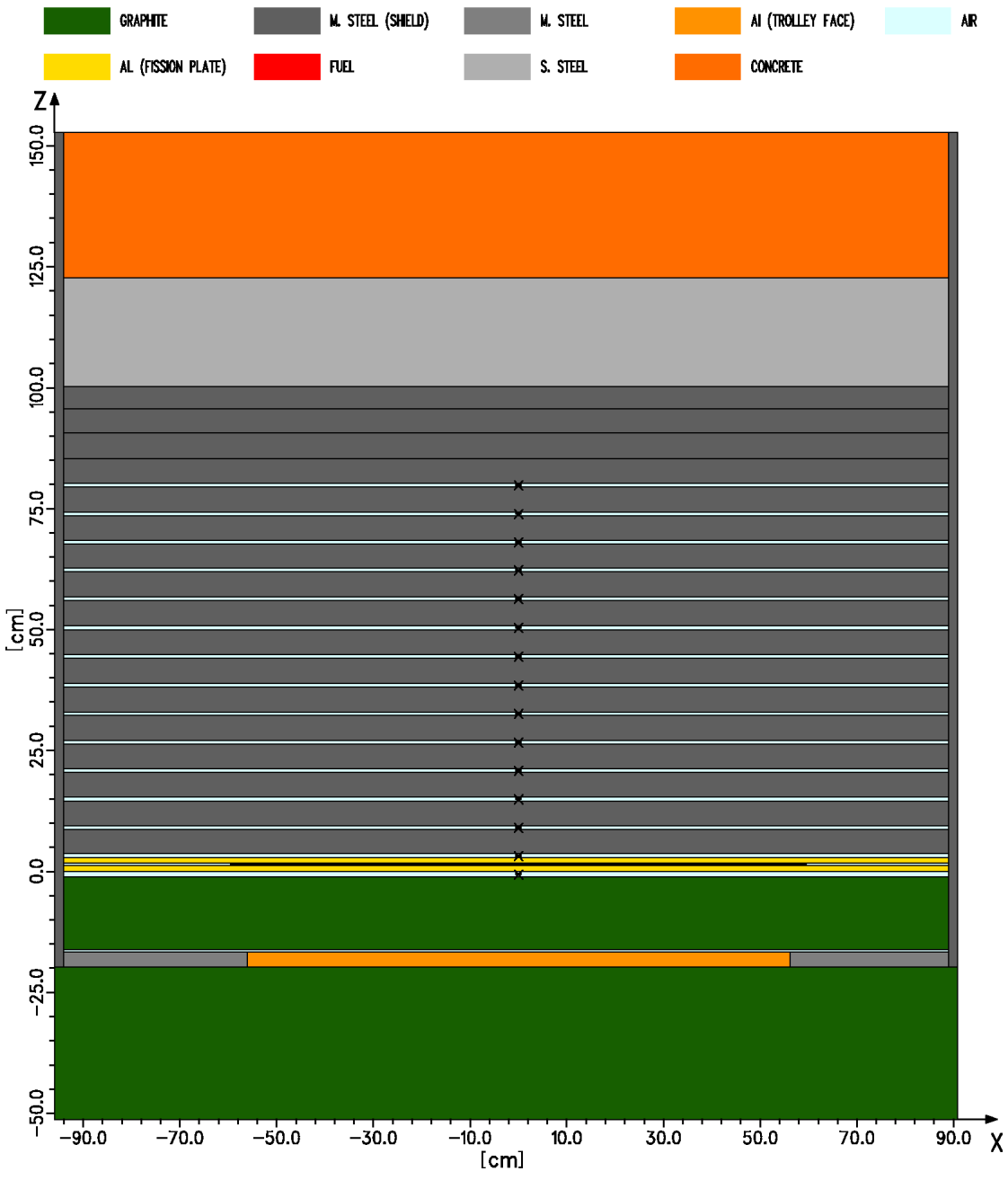

3.3 - Discussion of the Preliminary Results

The Iron-88 neutron dose calculated results for the four (see 2.3) threshold activation detectors, obtained through the BUGJEFF311.BOLIB and BUGLE-96 libraries, were compared with the corresponding experimental results. In the present preliminary work the epi-cadmium Au-197(n,γ)Au-198 reaction rates were not calculated (see 3.2).

The experimental dosimetric results were obtained in Iron-88 with four threshold activation dosimeters located in fourteen measurement positions. In particular the S-32(n,p)P-32 dosimeters were positioned in all the fourteen measurement positions located in the air gaps (see 2.3 and 3.2) between the mild steel slab components, the Rh-103(n,n')Rh-103m dosimeters in thirteen positions, the In-115(n,n')In-115m dosimeters in ten positions and the Al-27(n,α)Na-24 dosimeters only in four positions.

The calculated reaction rate results obtained with the flat weighting and 1/4 T RPV weighting neutron dosimeter cross sections are reported in Table 7 for Rh-103(n,n')Rh-103m, in Table 8 for In-115(n,n')In-115m, in Table 9 for S-32(n,p)P-32 and in Table 10 for Al-27(n,α)Na-24.
The dosimeter total experimental uncertainties at the specific measurement positions and at the confidence level of one standard deviation (1σ) were taken from the "General Description of the Experiment" document, included in the Iron-88 section of SINBAD REACTOR /3/.
The experimental reaction rates for all the four threshold activation dosimeters were respectively taken from the Table 8 of reference /2/ for sulphur, from the Table 9 for indium, from the Table 10 for rhodium and from the Table 12 for aluminium. It is underlined that the "as measured" experimental reaction rates reported in the previously cited tables contain a contribution from the NESTOR core neutron leakage background (see 2.3). Consequently, since the Calculated (C) reaction rates refer only to the neutrons produced in the fission plate, the "as measured" Experimental (E) reaction rate values in the C/E ratios are reduced by 2% to eliminate the NESTOR reactor background component in all the measurement positions for all the four threshold activation dosimeters, as recommended at page 2 of the Iron-88 /2/ report. All the calculated results reported in the previously cited Tables 7÷10 were obtained using the BUGJEFF311.BOLIB and the BUGLE-96 libraries together with the TORT-3.2 code in P_3-S_8 approximation.

The calculations using the BUGJEFF311.BOLIB library give the following results.
The Rh-103(n,n')Rh-103m calculated reaction rates present deviations from the corresponding experimental results contained within ±20% with a trend to overestimation, independently from the flat or 1/4 T RPV weighting neutron dosimeter cross sections.
With respect to the In-115(n,n')In-115m calculated reaction rates, they show deviations from the corresponding experimental results contained within ±15-20% with a trend to underestimation, independently from the flat or 1/4 T RPV weighting neutron dosimeter cross sections.
Concerning the S-32(n,p)P-32 calculated reaction rates, the results obtained with flat and 1/4 T RPV weighting neutron dosimeter cross sections give deviations from the corresponding experimental results included within ±15-20% with a systematic trend to underestimation.
Finally for the Al-27(n,α)Na-24 calculated reaction rates obtained with 1/4 T RPV weighting neutron dosimeter cross sections, overestimated deviations from the corresponding experimental results up to +30% are noted. It is underlined that only for this type of dosimeter, with the highest effective neutron energy threshold of 7.30 MeV, we have

meaningful differences between the results obtained with the flat weighting dosimeter cross sections and those calculated with the 1/4 T RPV weighting dosimeter cross sections.
In fact with the flat weighting dosimeter cross sections, the deviations from the corresponding experimental results are systematically overestimated by about 8%, with respect to the corresponding results obtained with the 1/4 T RPV weighting dosimeter cross sections.

Concerning the BUGLE-96 results, it is noted that, for the three lower effective energy threshold dosimeters Rh-103(n,n')Rh-103m, In-115(n,n')In-115m and S-32(n,p)P-32, the BUGLE-96 results are systematically lower with respect to the corresponding BUGJEFF311.BOLIB results. On the contrary, for the Al-27(n,α)Na-24 dosimeters with the highest effective neutron energy threshold, the BUGLE-96 results are higher with respect to the corresponding BUGJEFF311.BOLIB results.

In conclusion the BUGJEFF311.BOLIB library permitted to obtain calculated results, for the three lower effective energy threshold dosimeters Rh-103(n,n')Rh-103m, In-115(n,n')In-115m and S-32(n,p)P-32, characterized by deviations from the corresponding experimental results of ± 15-20%. Only the calculations with the Al-27(n,α)Na-24 neutron dosimeter cross sections give always results excessively overestimated (up to about 30%) with respect to the corresponding experimental results.

Table 7

Iron-88 - Summary of Experimental (E) and Calculated (C)
Rh-103(n,n')Rh-103m Reaction Rates along the Horizontal Z Axis.

Rh-103(n,n') Flat Weighting

Position	Shield Thickness [cm]	Exp.RR[a] as Measured	Total Error (1σ) [%]	Exp.RR[b] without Background (E)	BUGJEFF311 Calculated RR[a] (C)	C/E	BUGLE-96 Calculated RR[a] (C)	C/E
A2	0.00	3.35e-16	5.1	3.28e-16	3.41610E-16	1.04	3.42973E-16	1.04
A3	5.10	1.42e-16	5.2	1.39e-16	1.50060E-16	1.08	1.49423E-16	1.07
A4	10.22	7.78e-17	5.1	7.62e-17	8.67702E-17	1.14	8.58214E-17	1.13
A5	15.34	4.70e-17	5.1	4.61e-17	5.27376E-17	1.14	5.18212E-17	1.13
A6	20.44	2.86e-17	5.2	2.80e-17	3.32228E-17	1.19	3.24300E-17	1.16
A7	25.64	1.82e-17	5.1	1.78e-17	2.12622E-17	1.19	2.06113E-17	1.16
A8	30.79	1.20e-17	5.1	1.18e-17	1.39108E-17	1.18	1.33901E-17	1.14
A9	35.99	7.97e-18	5.2	7.81e-18	9.18976E-18	1.18	8.78199E-18	1.12
A10	41.19	5.48e-18	5.2	5.37e-18	6.13757E-18	1.14	5.82288E-18	1.08
A11	46.44	3.84e-18	5.2	3.76e-18	4.11633E-18	1.09	3.87668E-18	1.03
A12	51.62	2.68e-18	5.1	2.63e-18	2.79215E-18	1.06	2.61051E-18	0.99
A13	56.69	1.89e-18	5.2	1.85e-18	1.91861E-18	1.04	1.78095E-18	0.96
A14	61.81	1.34e-18	5.1	1.31e-18	1.31908E-18	1.00	1.21543E-18	0.93
A15	66.99	-	-	-	-	-	-	-

[a] RR = Reaction Rates in units of reactions per second per atom at 30 kW of NESTOR reactor power.
[b] RR Background are the experimental reaction rates reduced by 2% to eliminate the NESTOR reactor background component. These data are used to obtain the C/E ratios.

Rh-103(n,n') 1/4 T RPV Weighting

Position	Shield Thickness [cm]	Exp.RR[a] as Measured	Total Error (1σ) [%]	Exp.RR[b] without Background (E)	BUGJEFF311 Calculated RR[a] (C)	C/E	BUGLE-96 Calculated RR[a] (C)	C/E
A2	0.00	3.35e-16	5.1	3.28e-16	3.40180E-16	1.04	3.41214E-16	1.04
A3	5.10	1.42e-16	5.2	1.39e-16	1.49111E-16	1.07	1.48200E-16	1.06
A4	10.22	7.78e-17	5.1	7.62e-17	8.61097E-17	1.13	8.49630E-17	1.11
A5	15.34	4.70e-17	5.1	4.61e-17	5.22841E-17	1.14	5.12326E-17	1.11
A6	20.44	2.86e-17	5.2	2.80e-17	3.29125E-17	1.17	3.20303E-17	1.14
A7	25.64	1.82e-17	5.1	1.78e-17	2.10523E-17	1.18	2.03440E-17	1.14
A8	30.79	1.20e-17	5.1	1.18e-17	1.37686E-17	1.17	1.32114E-17	1.12
A9	35.99	7.97e-18	5.2	7.81e-18	9.09382E-18	1.16	8.66324E-18	1.11
A10	41.19	5.48e-18	5.2	5.37e-18	6.07277E-18	1.13	5.74394E-18	1.07
A11	46.44	3.84e-18	5.2	3.76e-18	4.07266E-18	1.08	3.82434E-18	1.02
A12	51.62	2.68e-18	5.1	2.63e-18	2.76251E-18	1.05	2.57555E-18	0.98
A13	56.69	1.89e-18	5.2	1.85e-18	1.89828E-18	1.02	1.75733E-18	0.95
A14	61.81	1.34e-18	5.1	1.31e-18	1.30516E-18	0.99	1.19947E-18	0.91
A15	66.99	-	-	-	-	-	-	-

[a] RR = Reaction Rates in units of reactions per second per atom at 30 kW of NESTOR reactor power.
[b] RR Background are the experimental reaction rates reduced by 2% to eliminate the NESTOR reactor background component. These data are used to obtain the C/E ratios.

Table 8

Iron-88 - Summary of Experimental (E) and Calculated (C)
In-115(n,n')In-115m Reaction Rates along the Horizontal Z Axis.

In-115(n,n') Flat Weighting

Position	Shield Thickness [cm]	Exp.RR[a] as Measured	Total Error (1σ) [%]	Exp.RR[b] without Background (E)	BUGJEFF311 Calculated RR[a] (C)	C/E	BUGLE-96 Calculated RR[a] (C)	C/E
A2	0.00	7.02e-17	4.5	6.88e-17	7.15052E-17	1.04	7.17707E-17	1.04
A3	5.10	2.40e-17	4.5	2.35e-17	2.27472E-17	0.97	2.26078E-17	0.96
A4	10.22	1.06e-17	4.5	1.04e-17	1.02723E-17	0.99	1.01409E-17	0.98
A5	15.34	5.14e-18	4.5	5.04e-18	4.89770E-18	0.97	4.80992E-18	0.95
A6	20.44	2.53e-18	4.5	2.48e-18	2.43008E-18	0.98	2.37515E-18	0.96
A7	25.64	1.32e-18	4.5	1.29e-18	1.22881E-18	0.95	1.19474E-18	0.92
A8	30.79	7.21e-19	4.5	7.07e-19	6.43201E-19	0.91	6.21436E-19	0.88
A9	35.99	3.93e-19	4.6	3.85e-19	3.43725E-19	0.89	3.29522E-19	0.86
A10	41.19	2.21e-19	4.6	2.17e-19	1.88652E-19	0.87	1.79248E-19	0.83
A11	46.44	1.28e-19	4.7	1.25e-19	1.05383E-19	0.84	9.91191E-20	0.79
A12	51.62	-	-	-	-	-	-	-
A13	56.69	-	-	-	-	-	-	-
A14	61.81	-	-	-	-	-	-	-
A15	66.99	-	-	-	-	-	-	-

[a] RR = Reaction Rates in units of reactions per second per atom at 30 kW of NESTOR reactor power.
[b] RR Background are the experimental reaction rates reduced by 2% to eliminate the NESTOR reactor background component. These data are used to obtain the C/E ratios.

In-115(n,n') 1/4 T RPV Weighting

Position	Shield Thickness [cm]	Exp.RR[a] as Measured	Total Error (1σ) [%]	Exp.RR[b] without Background (E)	BUGJEFF311 Calculated RR[a] (C)	C/E	BUGLE-96 Calculated RR[a] (C)	C/E
A2	0.00	7.02e-17	4.5	6.88e-17	7.11248E-17	1.03	7.13646E-17	1.04
A3	5.10	2.40e-17	4.5	2.35e-17	2.25498E-17	0.96	2.23923E-17	0.95
A4	10.22	1.06e-17	4.5	1.04e-17	1.01599E-17	0.98	1.00171E-17	0.96
A5	15.34	5.14e-18	4.5	5.04e-18	4.83372E-18	0.96	4.73912E-18	0.94
A6	20.44	2.53e-18	4.5	2.48e-18	2.39330E-18	0.97	2.33429E-18	0.94
A7	25.64	1.32e-18	4.5	1.29e-18	1.20770E-18	0.93	1.17123E-18	0.91
A8	30.79	7.21e-19	4.5	7.07e-19	6.30919E-19	0.89	6.07748E-19	0.86
A9	35.99	3.93e-19	4.6	3.85e-19	3.36548E-19	0.87	3.21528E-19	0.83
A10	41.19	2.21e-19	4.6	2.17e-19	1.84412E-19	0.85	1.74534E-19	0.81
A11	46.44	1.28e-19	4.7	1.25e-19	1.02867E-19	0.82	9.63309E-20	0.77
A12	51.62	-	-	-	-	-	-	-
A13	56.69	-	-	-	-	-	-	-
A14	61.81	-	-	-	-	-	-	-
A15	66.99	-	-	-	-	-	-	-

[a] RR = Reaction Rates in units of reactions per second per atom at 30 kW of NESTOR reactor power.
[b] RR Background are the experimental reaction rates reduced by 2% to eliminate the NESTOR reactor background component. These data are used to obtain the C/E ratios.

Table 9

Iron-88 - Summary of Experimental (E) and Calculated (C)
S-32(n,p)P-32 Reaction Rates along the Horizontal Z Axis.

S-32(n,p) Flat Weighting

Position	Shield Thickness [cm]	Exp.RR[a] as Measured	Total Error (1σ) [%]	Exp.RR[b] without Background (E)	BUGJEFF311 Calculated RR[a] (C)	C/E	BUGLE-96 Calculated RR[a] (C)	C/E
A2	0.00	2.02e-17	6.5	1.98e-17	1.83602E-17	0.93	1.84440E-17	0.93
A3	5.10	4.29e-18	6.5	4.20e-18	3.74140E-18	0.89	3.68026E-18	0.88
A4	10.22	1.40e-18	6.5	1.37e-18	1.26967E-18	0.93	1.22978E-18	0.90
A5	15.34	5.12e-19	6.5	5.02e-19	4.65183E-19	0.93	4.45076E-19	0.89
A6	20.44	1.91e-19	6.5	1.87e-19	1.74899E-19	0.93	1.65574E-19	0.88
A7	25.64	7.13e-20	6.5	6.99e-20	6.55344E-20	0.94	6.14629E-20	0.88
A8	30.79	2.70e-20	6.6	2.65e-20	2.48779E-20	0.94	2.31380E-20	0.87
A9	35.99	1.03e-20	6.5	1.01e-20	9.35837E-21	0.93	8.63658E-21	0.86
A10	41.19	3.93e-21	6.5	3.85e-21	3.53309E-21	0.92	3.23855E-21	0.84
A11	46.44	1.49e-21	6.5	1.46e-21	1.32126E-21	0.90	1.20369E-21	0.82
A12	51.62	5.73e-22	6.5	5.62e-22	5.01085E-22	0.89	4.54099E-22	0.81
A13	56.69	2.27e-22	6.9	2.22e-22	1.94247E-22	0.87	1.75282E-22	0.79
A14	61.81	8.53e-23	8.6	8.36e-23	7.47260E-23	0.89	6.72015E-23	0.80
A15	66.99	3.50e-23	21.	3.43e-23	2.84802E-23	0.83	2.55487E-23	0.74

[a] RR = Reaction Rates in units of reactions per second per atom at 30 kW of NESTOR reactor power.
[b] RR Background are the experimental reaction rates reduced by 2% to eliminate the NESTOR reactor background component. These data are used to obtain the C/E ratios.

S-32(n,p) 1/4 T RPV Weighting

Position	Shield Thickness [cm]	Exp.RR[a] as Measured	Total Error (1σ) [%]	Exp.RR[b] without Background (E)	BUGJEFF311 Calculated RR[a] (C)	C/E	BUGLE-96 Calculated RR[a] (C)	C/E
A2	0.00	2.02e-17	6.5	1.98e-17	1.82053E-17	0.92	1.82829E-17	0.92
A3	5.10	4.29e-18	6.5	4.20e-18	3.70835E-18	0.88	3.64734E-18	0.87
A4	10.22	1.40e-18	6.5	1.37e-18	1.25807E-18	0.92	1.21856E-18	0.89
A5	15.34	5.12e-19	6.5	5.02e-19	4.60796E-19	0.92	4.40926E-19	0.88
A6	20.44	1.91e-19	6.5	1.87e-19	1.73197E-19	0.93	1.63992E-19	0.88
A7	25.64	7.13e-20	6.5	6.99e-20	6.48755E-20	0.93	6.08590E-20	0.87
A8	30.79	2.70e-20	6.6	2.65e-20	2.46191E-20	0.93	2.29034E-20	0.87
A9	35.99	1.03e-20	6.5	1.01e-20	9.25741E-21	0.92	8.54577E-21	0.85
A10	41.19	3.93e-21	6.5	3.85e-21	3.49346E-21	0.91	3.20308E-21	0.83
A11	46.44	1.49e-21	6.5	1.46e-21	1.30580E-21	0.89	1.18989E-21	0.81
A12	51.62	5.73e-22	6.5	5.62e-22	4.94951E-22	0.88	4.48620E-22	0.80
A13	56.69	2.27e-22	6.9	2.22e-22	1.91752E-22	0.86	1.73047E-22	0.78
A14	61.81	8.53e-23	8.6	8.36e-23	7.37139E-23	0.88	6.62906E-23	0.79
A15	66.99	3.50e-23	21.	3.43e-23	2.80710E-23	0.82	2.51778E-23	0.73

[a] RR = Reaction Rates in units of reactions per second per atom at 30 kW of NESTOR reactor power.
[b] RR Background are the experimental reaction rates reduced by 2% to eliminate the NESTOR reactor background component. These data are used to obtain the C/E ratios.

Table 10

Iron-88 - Summary of Experimental (E) and Calculated (C)
Al-27(n,α)Na-24 Reaction Rates along the Horizontal Z Axis.

Al-27(n,alpha) Flat Weighting

Position	Shield Thickness [cm]	Exp.RR[a] as Measured	Total Error (1σ) [%]	Exp.RR[b] without Background (E)	BUGJEFF311 Calculated RR[a] (C)	C/E	BUGLE-96 Calculated RR[a] (C)	C/E
A2	0.00	-	-	-	-	-	-	-
A3	5.10	2.23e-20	4.7	2.19e-20	2.88891E-20	1.32	2.92900E-20	1.34
A4	10.22	-	-	-	-	-	-	-
A5	15.34	2.55e-21	4.7	2.50e-21	3.27233E-21	1.31	3.35773E-21	1.34
A6	20.44	9.56e-22	4.7	9.37e-22	1.23792E-21	1.32	1.27643E-21	1.36
A7	25.64	3.56e-22	4.7	3.49e-22	4.76262E-22	1.37	4.92905E-22	1.41
A8	30.79	-	-	-	-	-	-	-
A9	35.99	-	-	-	-	-	-	-
A10	41.19	-	-	-	-	-	-	-
A11	46.44	-	-	-	-	-	-	-
A12	51.62	-	-	-	-	-	-	-
A13	56.69	-	-	-	-	-	-	-
A14	61.81	-	-	-	-	-	-	-
A15	66.99	-	-	-	-	-	-	-

[a] RR = Reaction Rates in units of reactions per second per atom at 30 kW of NESTOR reactor power.
[b] RR Background are the experimental reaction rates reduced by 2% to eliminate the NESTOR reactor background component. These data are used to obtain the C/E ratios.

Al-27(n,alpha) 1/4 T RPV Weighting

Position	Shield Thickness [cm]	Exp.RR[a] as Measured	Total Error (1σ) [%]	Exp.RR[b] without Background (E)	BUGJEFF311 Calculated RR[a] (C)	C/E	BUGLE-96 Calculated RR[a] (C)	C/E
A2	0.00	-	-	-	-	-	-	-
A3	5.10	2.23e-20	4.7	2.19e-20	2.71400E-20	1.24	2.74629E-20	1.26
A4	10.22	-	-	-	-	-	-	-
A5	15.34	2.55e-21	4.7	2.50e-21	3.08155E-21	1.23	3.15582E-21	1.26
A6	20.44	9.56e-22	4.7	9.37e-22	1.16749E-21	1.25	1.20151E-21	1.28
A7	25.64	3.56e-22	4.7	3.49e-22	4.49935E-22	1.29	4.64792E-22	1.33
A8	30.79	-	-	-	-	-	-	-
A9	35.99	-	-	-	-	-	-	-
A10	41.19	-	-	-	-	-	-	-
A11	46.44	-	-	-	-	-	-	-
A12	51.62	-	-	-	-	-	-	-
A13	56.69	-	-	-	-	-	-	-
A14	61.81	-	-	-	-	-	-	-
A15	66.99	-	-	-	-	-	-	-

[a] RR = Reaction Rates in units of reactions per second per atom at 30 kW of NESTOR reactor power.
[b] RR Background are the experimental reaction rates reduced by 2% to eliminate the NESTOR reactor background component. These data are used to obtain the C/E ratios.

4 - CONCLUSION

The ENEA-Bologna BUGJEFF311.BOLIB (JEFF-3.1.1 data) broad-group coupled (47 n + 20 γ) working cross section library in FIDO-ANISN format, specifically conceived for LWR shielding and pressure vessel dosimetry applications, was validated on the Iron-88 single material (iron) neutron shielding benchmark experiment, included in the SINBAD international database. This preliminary validation was performed through three-dimensional fixed source transport calculations in Cartesian (X,Y,Z) geometry using the ORNL TORT-3.2 discrete ordinates (S_N) code. The calculated reaction rates for four threshold activation detectors (Rh-103(n,n')Rh-103m, In-115(n,n')In-115m, S-32(n,p)P-32 and Al-27(n,α)Na-24) were obtained through the corresponding dosimeter cross section sets, derived from the IAEA IRDF-2002 dosimetry file, and were compared with the corresponding experimental results.
For the three dosimeters Rh-103(n,n')Rh-103m, In-115(n,n')In-115m and S-32(n,p)P-32 with lower effective neutron energy threshold, the BUGJEFF311.BOLIB library gave calculated results characterized by deviations of ± 15-20% from the corresponding experimental results. Only the calculations for the Al-27(n,α)Na-24 dosimeters with the highest effective neutron energy threshold produced results systematically and excessively overestimated (up to about 30%) with respect to the corresponding experimental results.
Taking into account the total experimental uncertainties at the confidence level of one standard deviation (1σ) of the Rh-103(n,n')Rh-103m, In-115(n,n')In-115m and S-32(n,p)P-32 dosimeters, the corresponding calculated reaction rate results presented in this paper exhibit good statistical consistency with the corresponding measurements. On the contrary, the calculated reaction rates for the Al-27(n,α)Na-24 dosimeters are always excessively overestimated (up to about 30%) with respect to the corresponding experimental results with their related uncertainties at the confidence level of 1σ.
Concerning the results obtained through the BUGLE-96 reference library, it is noted that, for the three lower effective neutron energy threshold dosimeters Rh-103(n,n')Rh-103m, In-115(n,n')In-115m and S-32(n,p)P-32, the results obtained using BUGLE-96 are systematically underestimated with respect to the corresponding results calculated with BUGJEFF311.BOLIB. On the contrary, for the Al-27(n,α)Na-24 dosimeters with the highest effective neutron energy threshold, the BUGLE-96 results are overestimated with respect to the corresponding BUGJEFF311.BOLIB results.

REFERENCES

/1/ M. Pescarini, V. Sinitsa, R. Orsi, M. Frisoni, BUGJEFF311.BOLIB - A JEFF-3.1.1 Broad-Group Coupled (47 n + 20 γ) Cross Section Library in FIDO-ANISN Format for LWR Shielding and Pressure Vessel Dosimetry Applications, ENEA-Bologna Technical Report UTFISSM-P9H6-002, May 12, 2011. ENEA-Bologna Technical Report UTFISSM-P9H6-002 Revision 1 published on March 14, 2013. Available from OECD-NEA Data Bank as NEA-1866/02 ZZ BUGJEFF311.BOLIB.

/2/ G.A. Wright, M.J. Grimstone, Benchmark Testing of JEF-2.2 Data for Shielding Applications: Analysis of the Winfrith Iron-88 Benchmark Experiment, AEA Report AEA-RS-1231, March 1993.

/3/ Radiation Shielding Integral Benchmark Archive Database (SINBAD), OECD-NEA Data Bank/ ORNL-RSICC, SINBAD REACTOR, NEA-1517, 2009 Edition.

/4/ I. Kodeli, E. Sartori, B. Kirk, SINBAD Shielding Benchmark Experiments Status and Planned Activities, The American Society's 14th Biennial Topical Meeting of the Radiation Protection and Shielding Division, Carlsbad, New Mexico, USA, April 3-6, 2006.

/5/ W.A. Rhoades, D.B. Simpson, The TORT Three-Dimensional Discrete Ordinates Neutron/Photon Transport Code (TORT Version 3), Oak Ridge, ORNL Report ORNL/TM-13221, October 1997.

/6/ O.Bersillon, L.R. Greenwood, P.J. Griffin, W. Mannhart, H.J. Nolthenius, R. Paviotti-Corcuera, K.I. Zolotarev, E.M. Zsolnay, International Reactor Dosimetry File 2002 (IRDF-2002), IAEA, Vienna, Austria, Technical Reports Series No. 452, 2006.

/7/ W.W. Engle, Jr., A Users Manual for ANISN, A One Dimensional Discrete Ordinates Transport Code with Anisotropic Scattering, ORNL K-1693, Updated June 6, 1973. Available from OECD-NEA Data Bank as CCC-254 ANISN-ORNL.

/8/ The JEFF-3.1.1 Nuclear Data Library, JEFF Report 22, OECD-NEA Data Bank, 2009.

/9/ The JEFF-3.1 Nuclear Data Library, JEFF Report 21, OECD-NEA Data Bank, 2006.

/10/ J.E. White, D.T. Ingersoll, R.Q. Wright, H.T. Hunter, C.O. Slater, N.M. Greene, R.E. MacFarlane, R.W. Roussin, Production and Testing of the Revised VITAMIN-B6 Fine-Group and the BUGLE-96 Broad-Group Neutron/Photon Cross-Section Libraries Derived from ENDF/B-VI.3 Nuclear Data, Oak Ridge, ORNL Report ORNL-6795/R1, NUREG/CR-6214, Revision 1, January 1995. VITAMIN-B6 library available from OECD-NEA Data Bank as DLC-0184 ZZ VITAMIN-B6. BUGLE-96 library available from OECD-NEA Data Bank as DLC-0185 ZZ BUGLE-96.

/11/ American National Standard, American Nuclear Society, Neutron and Gamma-Ray Cross Sections for Nuclear Radiation Protection Calculations for Nuclear Power Plants, ANSI/ANS-6.1.2-1999 (R2009).

12/ M.J. Armishaw, J. Butler, M.D. Carter, I.J Curl, A.K. McCracken, A transportable Neutron Spectrometer (TNS) for radiological applications, AEEW-M2365, 1986.

/13/ J.H. Baard, W.L. Zijp, H.J. Nolthenius, Nuclear Data Guide for Reactor Neutron Metrology, Kluwer Academic Publishers, 1989.

/14/ G. Hehn, A. Sohn, M. Mattes, G. Pfister, IKE Calculations of the OECD/NEA Benchmarks VENUS-1 and VENUS-3 for Computing Radiation Dose to Reactor Pressure Vessel and Internals, Universität Stuttgart, Institut für Kernenergetik und Energiesysteme, IKE 6 NEA 2, December 1997.

/15/ I.J Curl, CRISP - A Computer Code to Define Fission Plate Source Profiles, RPD/IJC/934.

/16/ P.F. Rose, ENDF/B-VI Summary Documentation, Brookhaven National Laboratory, BNL-NCS-17541 (ENDF-201) 4th Edition, October 1991.

/17/ M. Pescarini, V. Sinitsa, R. Orsi, VITJEFF311.BOLIB - A JEFF-3.1.1 Multigroup Coupled (199 n + 42 γ) Cross Section Library in AMPX Format for Nuclear Fission Applications, ENEA-Bologna Technical Report UTFISSM-P9H6-003, November 10, 2011. ENEA-Bologna Technical Report UTFISSM-P9H6-003 Revision 1 published on March 14, 2013. Available from OECD-NEA Data Bank as NEA-1869/01 ZZ VITJEFF311.BOLIB.

/18/ I.I. Bondarenko, M.N. Nikolaev, L.P. Abagyan, N.O. Bazaziants, Group Constants for Nuclear Reactors Calculations, Consultants Bureau, New York, 1964.

/19/ J. Butler, M.D. Carter, I.J. Curl, M.R. March, A.K. McCracken, M.F. Murphy, A. Packwood, The PCA-Replica Experiment Part I Winfrith Measurements and Calculations, UKAEA, AEE Winfrith Report AEEW-R 1736, January 1984.

/20/ J. Butler, The NESTOR Shielding and Dosimetry Improvement Programme NESDIP for PWR Applications, PRPWG/P (82)5, Internal UKAEA Document, November 1982.

/21/ L. Leenders, LWR-PVS Benchmark Experiment VENUS-3 (with Partial Shielded Assemblies) - Core Description and Qualification, Mol, SCK/CEN Report FCP/VEN/01, September 1, 1988.

/22/ DOORS3.1: One-, Two- and Three-Dimensional Discrete Ordinates Neutron/Photon Transport Code System, ORNL, RSIC Computer Code Collection CCC-650, August 1996. Available from OECD/NEA Data Bank as CCC-0650/04 DOORS-3.2A.

/23/ R. Orsi, BOT3P Version 5.3: A Pre/Post-Processor System for Transport Analysis, ENEA-Bologna Technical Report FPN-P9H6-011, October 22, 2008. Available from OECD-NEA Data Bank as NEA-1678/09 BOT3P-5.3.

/24/ R. Orsi, The ENEA-Bologna pre-post-Processor Package BOT3P for the DORT and TORT Transport Codes (Version 1.0 - December 1999), JEF/DOC-828, JEFF Working Group Meeting on Benchmark Testing, Data Processing and Evaluations, OECD-NEA Data Bank, Issy-les-Moulineaux, France, May 22-24, 2000.

/25/ R. Orsi, BOT3P: Bologna Transport Analysis Pre-Post-Processors Version 1.0, Nuclear Science and Engineering, Technical Note, Volume 142, pp. 349-354, 2002.

/26/ R. Orsi, BOT3P: Bologna Transport Analysis Pre-Post-Processors Version 3.0, Nuclear Science and Engineering, Technical Note, Volume 146, pp. 248-255, 2004.

/27/ MCBEND User Guide to Version 7, ANSWERS/MCBEND(91)7.

/28/ R. Orsi, ADEFTA Version 4.1: A Program to Calculate the Atomic Densities of a Compositional Model for Transport Analysis, ENEA-Bologna Technical Report FPN-P9H6-010, May 20, 2008. Available from OECD-NEA Data Bank as NEA-1708/06 ADEFTA 4.1.

/29/ J.K. Tuli, Nuclear Wallet Cards (6^{th} Edition), National Nuclear Data Centre, Brookhaven National Laboratory, Upton, New York 11973-5000, USA, January 2000.

/30/ R. Orsi, M. Pescarini, V. Sinitsa, Dosimetry Cross Section Processing from IRDF-2002 in the BUGLE-96 (47 n) Neutron Group Structure Using Flat and Updated Problem Dependent Neutron Spectra, ENEA-Bologna Technical Report UTFISSM-P9H6-006, May 9, 2012.